Chinese Chemical Letters 31 (2020) 2516–2519

Contents lists available at ScienceDirect

Chinese Chemical Letters

journal homepage: www.elsevier.com/locate/cclet

Communication

Photosensitizer conjugate-functionalized poly(hexamethylene guanidine) for potentiated broad-spectrum bacterial inhibition and enhanced biocompatibility

Fengfeng Xiao[a,b,c,1], Bing Cao[a,b,1], Liewei Wen[c], Yanhong Su[c], Meixiao Zhan[c], Ligong Lu[c,*], Xianglong Hu[a,b,**]

[a] MOE Key Laboratory of Laser Life Science & Institute of Laser Life Science, College of Biophotonics, South China Normal University, Guangzhou 510631, China
[b] Guangdong Provincial Key Laboratory of Laser Life Science, College of Biophotonics, South China Normal University, Guangzhou 510631, China
[c] Zhuhai Interventional Medical Center, Zhuhai Precision Medical Center, Zhuhai People's Hospital, Zhuhai Hospital Affiliated with Jinan University, Jinan University, Zhuhai 519000, China

ARTICLE INFO

Article history:
Received 22 May 2020
Received in revised form 26 June 2020
Accepted 29 June 2020
Available online 30 June 2020

Keywords:
Poly(hexamethylene guanidine)
Photodynamic therapy
Eosin-Y
Broad-spectrum bacterial
Inhibition
Biocompatibility

ABSTRACT

Pathogen infection is the main cause of human morbidity and death. Traditional antibiotics usually sterilize bacteria in chemical ways, which tends to develop serious antibiotic resistance. Cationic polymers exhibit good bacterial inhibition with less resistance, but often face severe cytotoxicity toward normal cells. The optimization of polymeric antimicrobials for enhanced bactericidal capacity and improved biocompatibility is quite meaningful. In addition, photodynamic therapy (PDT) is a therapeutic modality with less susceptibility to develop resistance. Herein, a typical commercial polymeric antimicrobial, polyhexamethylene guanidine (PHMG) was selected for current proof-of-concept optimization due to its excellent bactericidal capacity but moderate biocompatibility. Eosin-Y (EoS) was copolymerized to afford EoS-labeled polymer conjugates, poly(2-(dimethylamino) ethyl methacrylate-*co*-eosin), P(DMAEMA-*co*-EoS), which was conjugated with PHMG to afford a novel polymeric antimicrobial, P(DMAEMA-*co*-EoS)-*b*-PHMG-*b*-P(DMAEMA-*co*-EoS), noted as PEoS-PHMG. It could efficiently kill broad-spectrum bacteria by physical damage and photodynamic therapy. Compared with PHMG, the bacterial inhibition of PEoS-PHMG was potentiated after the functionalization. Furthermore, PEoS-PHMG exhibited low cytotoxicity and minimal hemolysis, which was demonstrated by cell viability assays toward LO2 cells and RAW 264.7 cells as well as hemolytic assays against red blood cells. These results confirmed that the resultant PEoS-PHMG could act as promising alternative antibacterial materials with excellent broad-spectrum bacterial inhibition and favorable biocompatibility.

Pathogenic bacteria can cause serious morbidity and have become a critical public healthcare problem [1,2]. Especially, the infections caused by multidrug-resistant bacteria, are a global burden resulting in huge human death in the hundreds of thousands every year [3,4]. The emergence of resistant and more virulent bacteria strains even surpasses the development of new antimicrobial agents and methods [5]. Therefore, it is extremely urgent to develop new materials and alternative treatment strategies to combat antibiotic resistance [6–9]. Although photodynamic therapy (PDT) [10–12], sonodynamic therapy (SDT) [13] and photothermal therapy (PTT) [14,15] are promising methods to solve the issue of bacterial resistance, each of these is frequently suffered from some typical shortcomings, such as low efficiencies, low laser penetration depth, and poor therapeutic efficacy of single treatment modality [16]. Hence, it is still challenging to develop efficient therapeutic methods for bacterial killing. Multimodal therapy, the combination of two or more different therapeutic modalities, has become a promising approach to enhance antibacterial efficiency [17,18].

Typically, antimicrobial photodynamic therapy, as a photoinduced therapy, has been successfully applied in epidermis microbial infection [19–21]. Antimicrobial photodynamic therapy possesses some advantages, including non-invasiveness, easy

* Corresponding author.
** Corresponding author at: MOE Key Laboratory of Laser Life Science & Institute of Laser Life Science, College of Biophotonics, South China Normal University, Guangzhou 510631, China.
E-mail addresses: luligong1969@126.com (L. Lu), xlhu@scnu.edu.cn, huxlong@mail.ustc.edu.cn (X. Hu).
[1] These authors contributed equally to this work.

https://doi.org/10.1016/j.cclet.2020.06.038
1001-8417/

operation, short treatment cycle, low side effects and overcoming of resistant bacteria [22–24]. Resistant bacteria can be easily destroyed due to indiscriminate photodynamic damage to bacterial components [25,26], which results from the generated reactive oxygen species (ROS) that are toxic toward cells and microbes [27]. Most photosensitizers show good antibacterial ability against Gram-positive bacteria, but they are insufficient to inhibit Gram-negative bacteria because of their distinct membrane structure [28,29]. Therefore, it is imperative to develop broad-spectrum antibacterial materials that can inhibit both Gram-positive and Gram-negative bacteria [30].

Polyhexamethylene guanidine (PHMG), an effective and broad-spectrum cationic polymeric bactericide, has been widely applied in many fields (Scheme 1a), including medicine [31,32], wound care [33], water treatment [34], food industry, paper making and so on [35]. The antimicrobial mechanism of PHMG is demonstrated that cationic polymers can rapidly adsorb onto the negatively charged cell surface, impair the cellular membrane, and increase the permeability of cytoplasmic membrane to *in-situ* result in the formation of local pores, the leakage of intracellular components and final bacterial death [36–39]. Importantly, the physical damage mechanism of PHMG is very different from traditional antibiotics [40,41]. Physical damage is promising to overcome the bacterial resistance [42–44]. Meantime, the terminal amino groups of PHMG provide reactive sites to conjugate with other functional units.

In this work, we reported an efficient polymeric antimicrobial of EoS photosensitizer conjugate-functionalized PHMG, P(DMAEMA-*co*-EoS)-*b*-PHMG-*b*-P(DMAEMA-*co*-EoS), noted as PEoS-PHMG, which was prepared from the amidation reaction of PHMG and P(DMAEMA-*co*-EoS). Owing to the conjugation with P(DMAEMA-*co*-EoS), the resulting PEoS-PHMG exhibited dual-modality inhibition, including physical damage to the microbes and concurrent photodynamic killing (Scheme 1). PEoS-PHMG behaved great antimicrobial activities against methicillin-resistant *Staphylococcus aureus* (MRSA) and typical Gram-negative bacteria. Additionally, the antimicrobial PEoS-PHMG had good biocompatibility and low toxicity to mammalian cells.

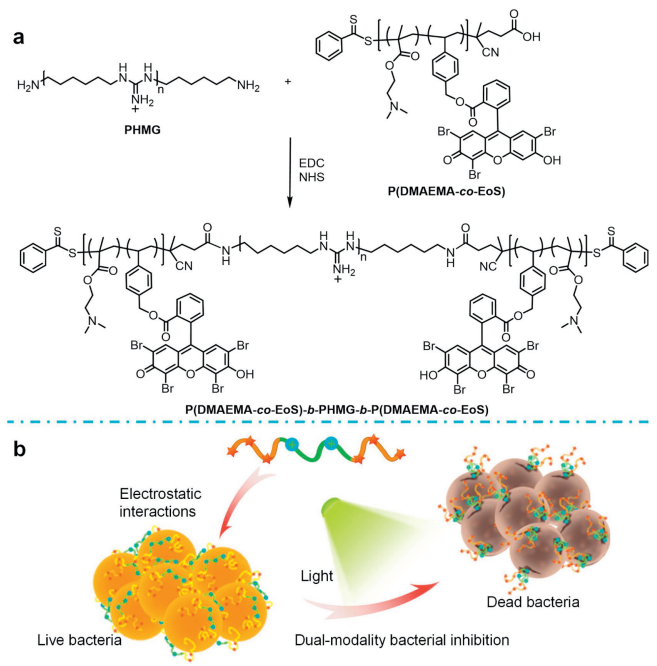

Scheme 1. Schematic illustration for (a) the synthesis of Eosin-Y polymer conjugate-modified PHMG, P(DMAEMA-*co*-EoS)-*b*-PHMG-*b*-P(DMAEMA-*co*-EoS), noted as PEoS-PHMG. (b) Dual-modality inhibition broad-spectrum bacteria *via* synergistic photodynamic inactivation and physical damage.

The fabrication of PEoS-PHMG was illustrated in Scheme 1a. The EoS-labeled polymer conjugate, P(DMAEMA-*co*-EoS) was prepared by facile reversible addition fragmentation chain transfer (RAFT) polymerization at first [45,46], which was characterized by ^{1}H NMR spectrum (Fig. S1 in Supporting information). The covalent conjugation between P(DMAEMA-*co*-EoS) and PHMG was achieved by the amidation reaction, affording PEoS-PHMG. The successful modification was characterized by typical FT-IR analysis (Fig. S2 in Supporting information), indicating the stretching vibration signals of C=N and C=O bonds in the resultant PEoS-PHMG. In addition, the UV–vis absorption spectra of Eosin-Y and PEoS-PHMG were recorded in water (Fig. 1a), indicating the absorbance red-shift from ~516 nm to ~536 nm for EoS moieties in PEoS-PHMG, which also confirmed the successful conjugation of P(DMAEMA-*co*-EoS) with PHMG. For the fluorescence emission spectra (Fig. 1b), similar emission red-shift from ~535 nm to ~562 nm for EoS moieties was also observed. In addition, the mean hydrodynamic diameter for the aqueous dispersion of PEoS-PHMG was determined to be ~12 nm by dynamic light scattering (DLS) analysis (Fig. S3 in Supporting information).

To verify the photodynamic potency of PEoS-PHMG, the single oxygen ($^1O_2$) generation potency was performed using 1,3-dipheny-lisobenzofuran (DPBF) as an indicator of $^1O_2$ [47,48]. DPBF can react with $^1O_2$ in a stoichiometric manner and form an irreversible endoperoxide to cause absorption decrease at ~410 nm [9]. As shown in Figs. 2a-c, after exposure to light, obvious absorption decreasing at ~410 nm was observed for Eosin-Y and PEoS-PHMG. More importantly, the consumption of DPBF for the PEoS-PHMG group was more quickly than that of Eosin-Y, suggesting enhanced $^1O_2$ yield for the resultant PEoS-PHMG. In contrast, no obvious absorbance decrease of DPBF was determined for PHMG. The normalized absorbance variation of different groups was also shown in Fig. 2d. These results indicated that PEoS-PHMG had the best ROS generation efficiency.

The antimicrobial activities of these materials were evaluated against clinically representative bacteria, including Gram-positive bacteria, *S. aureus*, MRSA and Gram-negative bacteria, *E. coli* and *P. aeruginosa*. Using a broth microdilution protocol [49], the minimum inhibitory concentrations (MIC) values were presented in Table 1 and Fig. 3, Figs. S5-S7 (Supporting information). These results demonstrated that PEoS-PHMG exhibited broad-spectrum antimicrobial activities against *S. aureus*, MRSA, *E. coli* and *P. aeruginosa* with MICs values of 0.5, 1, 1, 1 μmol/L under light irradiation, respectively. The MIC values of PEoS-PHMG were much lower than PHMG (1, 2, 4, 4 μmol/L) owing to that PHMG did not possess photodynamic antibacterial potency, only exhibiting physical inhibition for PHMG. Upon green light irradiation to activate the photodynamic process, the inhibition ability of Eosin-Y was still limited, especially for Gram-negative bacteria, because the generated ROS could not approach and attack bacteria membrane efficiently due to the short life time and limited action range of ROS [50,51]. Furthermore, Gram-negative bacteria possess

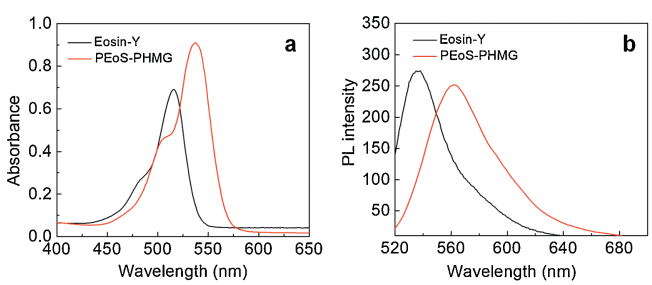

Fig. 1. (a) Absorbance spectra and (b) fluorescence emission spectra recorded for Eosin-Y and PEoS-PHMG, respectively. The excitation wavelength was set at 500 nm.

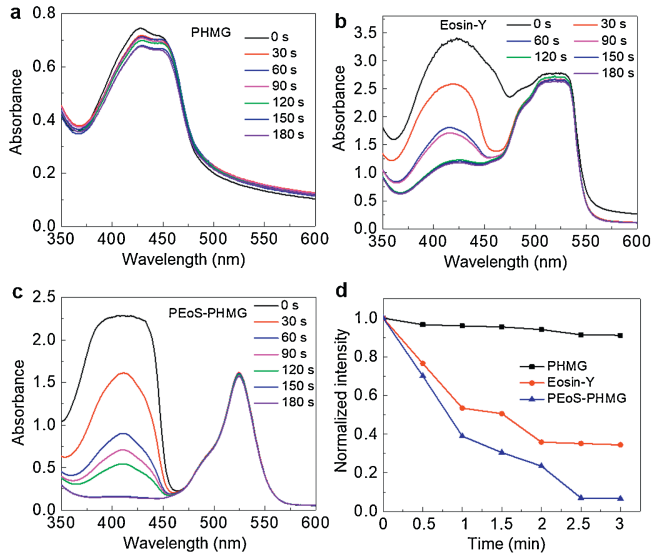

Fig. 2. *In vitro* evaluation of ROS generation upon light irradiation (520 ± 10 nm) at diverse durations for (a) PHMG, (b) Eosin-Y, and (c) PEoS-PHMG, respectively. DPBF was employed as a ROS indicator for ROS evaluation. (d) Normalized absorbance intensity at 410 nm recorded for (a)-(c), respectively.

Table 1
Minimum inhibition concentration (MIC) values evaluated for EoS, PHMG and PEoS-PHMG, respectively.

Samples		MIC (μmol/L)[a]			
		S. aureus	MRSA	*E. coli*	*P. aeruginosa*
EoS	Dark	>8	>8	>8	>8
	Light	4	4	>8	>8
PHMG	Dark	1	2	4	4
	Light	1	2	4	4
PEoS-PHMG	Dark	2	2	4	4
	Light	0.5	1	1	1

[a] MIC values were calculated by broth microdilution for *S. aureus*, MRSA, *E. coli* and *P. aeruginosa*, respectively.

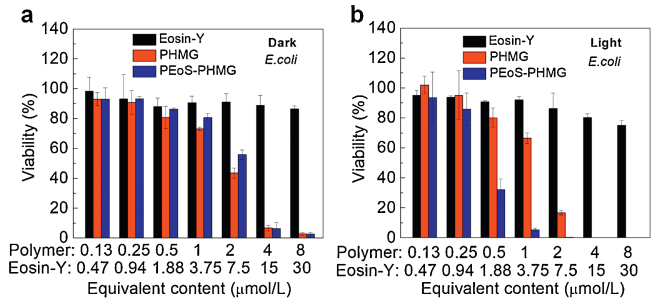

Fig. 3. Quantitative antibacterial tests were performed against *E. coli* upon incubation with different contents of Eosin-Y, PHMG, and PEoS-PHMG under dark (a) and light irradiation (b), respectively.

complicated cell envelopes with low permeability and extra defensive mechanisms [52,53]. Hence, the dual-modality antimicrobial potency of PEoS-PHMG exhibited highly effective broad-spectrum antibacterial ability.

To evaluate the synergistic bacterial inhibition of PEoS-PHMG *via* physical damage and photodynamic inactivation, typical combination index (CI) was utilized as a parameter *via* the Chou-Talalay method [54]. The CI value reflects the interaction effect of the dual-modality inhibition mechanisms. $0.3 < CI < 0.7$ indicates obvious synergism, $0.7 < CI < 0.85$ indicates moderate synergism [55]. The CI values of PEoS-PHMG with light irradiation for *S. aureus*, MRSA, *E. coli, P. aeruginosa* were calculated to be 0.375, 0.75, <0.375, and <0.375, respectively, indicating obvious synergy for *S. aurues, E.coli, P.aeruginosa*, and moderate effect for MRSA. These results demonstrated effective synergy for PEoS-PHMG via physical damage and PDT to inhibit broad-spectrum bacteria.

After that, to further verify the antibacterial effect of PEoS-PHMG, the OD_{600} values were recorded for the dispersion at different durations (Fig. 4). At the corresponding MIC value, there was no obvious OD_{600} rise in the whole process for the dispersion of *E. coli* upon incubation with PEoS-PHMG under light irradiation, exhibiting efficient inhibition. These results confirmed that the functionalization of PHMG further potentiated its broad-spectrum bacterial inhibition.

Furthermore, inhibition zone assay was performed in parallel for Eosin-Y, PHMG, and PEoS-PHMG, respectively (Fig. S4 in Supporting information). The area of inhibition zone reflected their relative inhibition potency. PEoS-PHMG possessed the largest inhibition zone upon light irradiation, suggesting favorable synergistical bacteria inhibition by PEoS-PHMG, which was much better than PHMG and Eosin-Y.

Apart from bacterial inhibition, the safety issue of antibacterial materials is critically important [56]. Then the hemolysis was analyzed for P(DMAEMA-*co*-EoS), PHMG and PEoS-PHMG, respectively. HC_{10}, the sample content that causes 10% hemolysis of mouse red blood cells (mRBCs) relative to that of control, was determined by incubation mRBCs with different content of the samples [57]. The HC_{10} value of PEoS-PHMG was determined to be over 32 μmol/L, and that of PHMG was detected to be higher than 16 μmol/L (Fig. 5). Hence, the blood safety of PEoS-PHMG was further enhanced for PHMG after modification [58,59]. The presence of hydrophilic P(DMAEMA-*co*-EoS) with less positive charge probably contributed to the minimal hemolysis of PEoS-PHMG [60,61].

In vitro cell viability was tested for two kinds of cell lines after incubation with these diverse samples. Cell counting kit-8 (CCK-8) assays were performed for two series of samples upon incubation with LO2 cells and RAW 264.7 cells for 24 h (Fig. 6). PEoS-PHMG showed undetectable toxicity toward both LO2 and RAW 264.7 cells even up to 8 μmol/L, approximately 2∼4-fold compared to their corresponding MIC values. The results demonstrated that the functionalized PEoS-PHMG had good antibacterial selectivity, which was toxic to bacteria but minimally harmful to mammalian cells.

In summary, a broad-spectrum polymeric antimicrobial, PEoS-PHMG, was developed to achieve dual-modality bacterial inhibition *via* photodynamic inactivation and physical damage. Compared with native PHMG, current photosensitizer conjugate-functionalized PHMG exhibited excellent bacterial inhibition and enhanced biocompatibility with minimal cytotoxicity toward mammalian cells. Herein, the photodynamic functionalization of PHMG is a promising strategy to exploit novel polymeric antimicrobials in biomedicine.

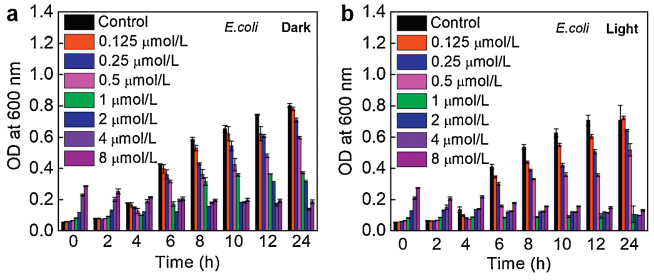

Fig. 4. Time-dependent growth inhibition of *E. coli* after incubation with PEoS-PHMG (a) at dark and (b) light irradiation, respectively.

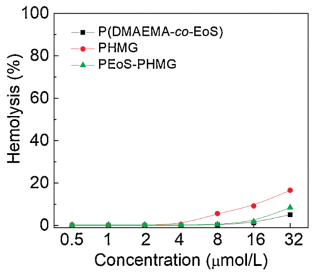

Fig. 5. Hemolysis activity analyzed for P(DMAEMA-*co*-EoS), PHMG and PEoS-PHMG, respectively.

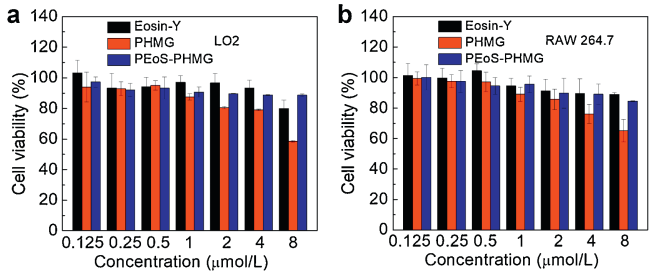

Fig. 6. *In vitro* cell viability of (a) LO2 cells and (b) RAW 264.7 cells after 24 h incubation with Eosin-Y, PHMG, and PEoS-PHMG at various contents.

Declaration of competing interest

The authors declare that they have no known competing financial interests or personal relationships that could have appeared to influence the work reported in this paper.

Acknowledgments

This work was supported by the Natural Science Foundation for Distinguished Young Scholars of Guangdong Province (No. 2016A030306013), the Pearl River Young Talents Program of Science and Technology in Guangzhou (No. 201906010047) and the National Key Research and Development Program of China (No. 2017YFA0205200)

Appendix A. Supplementary data

Supplementary material related to this article can be found, in the online version, at doi:https://doi.org/10.1016/j.cclet.2020.06.038.

References

[1] J. Zhou, G.B. Qi, H. Wang, J. Mater. Chem. B: Mater. Biol. Med. 4 (2016) 4855–4861.
[2] R. Yin, T. Agrawal, U. Khan, et al., Nanomedicine 10 (2015) 2379–2404.
[3] A.S. Abd-El-Aziz, C. Agatemor, N. Etkin, et al., Biomacromolecules 16 (2015) 3694–3703.
[4] L.J. Shallcross, S.J. Howard, T. Fowler, S.C. Davies, Philos. Trans. R. Soc. B 370 (2015)20140082.
[5] A. Reinhardt, I. Neundorf, Int. J. Mol. Sci. 17 (2016) 701.
[6] K.H. Wu, Y.C. Chang, J.C. Wang, Mater. Express 9 (2019) 970–977.
[7] A. Sun, X.Y. He, L. Li, et al., NPG Asia Mater. 12 (2020) 25.
[8] X.F. Luo, Y.J. Liu, Z.D. Qin, et al., J. Biomed. Nanotechnol. 14 (2018) 601–608.
[9] F. Xu, M. Hu, C. Liu, S.K. Choi, Biomater. Sci. 5 (2017) 678–685.
[10] X.J. Fu, Y. Fang, M. Yao, Biomed Res. Int. 2013 (2013) 159157.
[11] D. Hu, Y. Deng, F. Jia, Q. Jin, J. Ji, ACS Nano 14 (2020) 347–359.
[12] K. Liu, Y. Liu, Y. Yao, et al., Angew. Chem. Int. Ed. 52 (2013) 8285–8289.
[13] D. Costley, H. Nesbitt, N. Ternan, et al., Int. J. Antimicrob. Agents 49 (2017) 31–36.
[14] X. Huang, G. Chen, J. Pan, et al., J. Mater. Chem. B: Mater. Biol. Med. 4 (2016) 6258–6270.
[15] X. Guo, B. Cao, C. Wang, S. Lu, X. Hu, Nanoscale 12 (2020) 7651–7659.
[16] Y. Liu, H.C. van der Mei, B. Zhao, et al., Adv. Funct. Mater. 27 (2017) 1701974.
[17] M. Yin, Z. Li, E. Ju, et al., Chem. Commun. (Camb.) 50 (2014) 10488–10490.
[18] F.E. Akram, T. El-Tayeb, K. Abou-Aisha, M. El-Azizi, Ann. Clin. Microbiol. Antimicrob. 15 (2016) 48.
[19] M. van Oosten, M. Hahn, L.M. Crane, et al., FEMS Microbiol. Rev. 39 (2015) 892–916.
[20] G. Fila, K. Kasimova, Y. Arenas, et al., Front. Microbiol. 7 (2016) 1258.
[21] J. Xia, W. Wang, X. Hai, et al., Chin. Chem. Lett. 30 (2019) 421–424.
[22] L. Yang, P. Gao, Y. Huang, et al., Chin. Chem. Lett. 30 (2019) 1293–1296.
[23] T. Maisch, Lasers Med. Sci. 22 (2007) 83–91.
[24] X. Liu, M. Li, T. Han, et al., J. Am. Chem. Soc. 141 (2019) 11259–11268.
[25] H. Bai, F. Lv, L. Liu, S. Wang, Chemistry 22 (2016) 11114–11121.
[26] F. Vatansever, W.C. de Melo, P. Avci, et al., FEMS Microbiol. Rev. 37 (2013) 955–989.
[27] L. Chen, H. Bai, J.F. Xu, S. Wang, X. Zhang, ACS Appl. Mater. Interfaces 9 (2017) 13950–13957.
[28] X. Ragas, D. Sanchez-Garcia, R. Ruiz-Gonzalez, et al., J. Med. Chem. 53 (2010) 7796–7803.
[29] J. Chen, F. Wang, Q. Liu, J. Du, Chem. Commun. (Camb.) 50 (2014) 14482–14493.
[30] X.K. Ding, S. Duan, X.J. Ding, R.H. Liu, F.J. Xu, Adv. Funct. Mater. 28 (2018) 1802140.
[31] C. Kratzer, S. Tobudic, W. Graninger, A. Buxbaum, A. Georgopoulos, J. Hosp. Infect. 63 (2006) 316–322.
[32] M. Rosin, A. Welk, O. Bernhardt, et al., J. Clin. Periodontol. 28 (2001) 1121–1126.
[33] M.K. Oule, R. Azinwi, A.M. Bernier, et al., J. Med. Microbiol. 57 (2008) 1523–1528.
[34] J.M. Kusnetsov, A.I. Tulkki, H.E. Ahonen, P.J. Martikainen, J. Appl. Microbiol. 82 (1997) 763–768.
[35] Y. Guan, H. Xiao, H. Sullivan, A. Zheng, Carbohydr. Polym. 69 (2007) 688–696.
[36] P. Gilbert, L.E. Moore, J. Appl. Microbiol. 99 (2005) 703–715.
[37] Y. Wu, J. Bai, K. Zhong, Y. Huang, H. Gao, Food Chem. 218 (2017) 463–470.
[38] Z. Liang, M. Zhu, Y.W. Yang, H. Gao, Polym. Advan. Technol. 25 (2014) 117–122.
[39] Q. Cai, S. Yang, C. Zhang, et al., ACS Appl. Mater. Interfaces 10 (2018) 38506–38516.
[40] G.B. Qi, D. Zhang, F.H. Liu, Z.Y. Qiao, H. Wang, Adv. Mater. 29 (2017) 1703461.
[41] Q. Zeng, Y. Zhu, B. Yu, et al., Biomacromolecules 19 (2018) 2805–2811.
[42] A. Azizi, S. Mousavian, S. Taheri, et al., Photodiagn. Photodyn. Ther. 21 (2018) 357–362.
[43] Y.Y. Huang, A. Wintner, P.C. Seed, et al., Sci. Rep. 8 (2018) 7257.
[44] H. Sun, Y. Hong, Y. Xi, et al., Biomacromolecules 19 (2018) 1701–1720.
[45] K.L. Zhu, G.H. Liu, J.M. Hu, S.Y. Liu, Biomacromolecules 18 (2017) 2571–2582.
[46] G.H. Liu, J.M. Hu, G.Q. Zhang, S.Y. Liu, Bioconjug. Chem. 26 (2015) 1328–1338.
[47] M. Yin, Z. Li, L. Zhou, et al., Nanotechnology 27 (2016) 125601.
[48] A. Gomes, E. Fernandes, J.L. Lima, J. Biochem, Biophys. Methods. 65 (2005) 45–80.
[49] I. Wiegand, K. Hilpert, R.E.W. Hancock, Nat. Protoc. 3 (2008) 163–175.
[50] S. Perni, P. Prokopovich, J. Pratten, I.P. Parkin, M. Wilson, Photochem. Photobiol. Sci. 10 (2011) 712–720.
[51] Y. Guo, S. Rogelj, P. Zhang, Nanotechnology 21 (2010) 065102.
[52] Y.M. Li, X.L. Hu, S.D. Tian, et al., Biomaterials 35 (2014) 1618–1626.
[53] X. Hu, X. Zhao, B. He, et al., Research 2018 (2018) 12.
[54] Y. Zhu, C. Xu, N. Zhang, et al., Adv. Funct. Mater. 28 (2018) 1706709.
[55] C. Wu, Q. He, A. Zhu, et al., ACS Appl. Mater. Interfaces 6 (2014) 21615–21623.
[56] B. Cao, F. Xiao, D. Xing, X. Hu, Small 14 (2018) 1802008.
[57] Y. Yu, F. Bu, H. Zhou, et al., Mater. Chem. Front. (2020), doi:http://dx.doi.org/10.1039/D1030QM00255K.
[58] H. Du, Y. Wang, X. Yao, et al., Polym. Chem. 7 (2016) 5620–5624.
[59] C. Zhang, Z. Ying, Q. Luo, et al., J. Polym. Sci.: Polym. Chem. Ed. 55 (2017) 2027–2035.
[60] W. Chin, C. Yang, V.W.L. Ng, et al., Macromolecules 46 (2013) 8797–8807.
[61] K. Saha, D.F. Moyano, V.M. Rotello, Mater. Horiz. 1 (2014) 102–105.